

# Densification Behavior of Ag-Graphene Composites Prepared by Low-pressure Compressing and Vacuum Sintering

Wang Song, Zheng Tingting, Xie Ming, Li Aikun, Hou Pan

State Key Laboratory of Advanced Technologies for Comprehensive Utilization of Platinum Metals, Kunming Institute of Precious Metals, Kunming 650106, China

**Abstract:** In order to clarify the densification behavior of new Ag-graphene composites prepared by low-pressure compressing and vacuum sintering, Ag-graphene mixed powders with different graphene contents from 0.5 wt% to 2.0 wt% were prepared by 24 h of ball milling and subsequently double action compressed and vacuum sintered. The densities of composites were measured after compressing and sintering, and the compressibility and sinterability of the composites at varying compaction pressures and sintering temperatures were also investigated. The results show that the compaction data of all Ag-graphene powders are fitted to the Balshin equation. The densification parameter ( $K$  values) increases with the increase of the graphene contents which indicates the increase of plastic deformation capacity. The Ag-0.5wt% graphene composite has the best sinterability. The composite with 1.5 wt% graphene exhibit much enhanced mechanical properties, whose, a tensile strength reaches to 252 MPa.

**Key words:** composites; Ag-graphene; densification behavior; sinterability; low-pressure compressing

In recent years, graphene has emerged as new reinforcement material in metal-based composites with excellent properties beyond any traditional reinforcement particles such as oxide, carbide, graphite and intermetallic compound<sup>[1-4]</sup>. Experimental results on graphene reveal Young's modulus of 1 TPa, a tensile strength of 130 GPa and a low density of 2.2 g/cm<sup>3</sup><sup>[5,6]</sup>. These superior mechanical properties combined with low density make graphene suitable as a reinforcement for metal-based composites<sup>[7-10]</sup>.

Researches on metal-based composites reinforced with graphene have been significantly growing over the past few years, focusing on contribution of graphene in improvement of composite mechanical, thermal and electrical contact performances. Sharma et al<sup>[11]</sup> demonstrated a surface modification of pure Al by graphene impregnation through a novel powder metallurgy assisted friction surfacing process. Composites prepared at relatively lower tool rotational speed with low content of graphene in the tool are found to

have optimum mechanical properties with a homogeneous distribution of graphene in Al matrix. The nano-hardness of the surface composite is increased by 100% after impregnation of graphene nano platelets with an optimum set of parameters. Gao et al<sup>[12]</sup> fabricated Cu-graphene composites by powder metallurgy and realized the homogeneous dispersion of graphene in the Cu matrix composites. The ultimate tensile strength and thermal conductivity of the composites initially increase and later decrease with the increase of the graphene content. However, the elongation to fracture of the composite gradually decreases. Wang et al<sup>[13]</sup> prepared Ag-graphene electrical contact composites by powder metallurgy. The highest electrical conductivity value of 84.5%IACS can be accomplished when the content of the graphene is 0.5 wt% in Ag matrix. When the amount of the graphene is higher than 2.0 wt%, the declining rate in hardness significantly increases. The Ag-1.5wt%Graphene electrical contact composite displays the best anti-arc ero-

Received date: November 25, 2018

Foundation item: National Natural Science Foundation of China (51707087); Applied Basic Research Programs of Yunnan Province (2018FB094)

Corresponding author: Xie Ming, Ph. D., Professor, State Key Laboratory of Advanced Technologies for Comprehensive Utilization of Platinum Metals, Kunming Institute of Precious Metals, Kunming 650106, P. R. China, Tel: 0086-871-68328842, E-mail: powder@ipm.com.cn

Copyright © 2019, Northwest Institute for Nonferrous Metal Research. Published by Science Press. All rights reserved.

sion performance.

Powder metallurgy technology could produce uniform dispersion of the graphene in the metal matrix which was confirmed by previous researchers<sup>[14,15]</sup>. However, little information is available on the densification behavior of metal-based composites reinforced with graphene in literature. In the present paper, Ag-graphene mixed powders with different graphene contents from 0.5wt% to 2.0 wt% were prepared by ball milling for 24 h and subsequently double action compressed with low-pressure and vacuum sintered. The densities of composites were measured after compressing and sintering, and the compressibility and sinterability of the composites at varying compaction pressures and sintering temperatures were also investigated.

## 1 Experiment

The graphene was purchased from Chengdu Organic Chemistry Co. Ltd, China, which consisted of platelets with the morphology of irregular shaped flakes, as shown in Fig.1a. Atomized commercial-purity silver powders with 99.95% in purity, 10~50  $\mu\text{m}$  in diameter and spherical shape were produced by Sino-platinum Metals Co. Ltd, China, as shown in Fig.1b. Ag-graphene mixed powders with different graphene contents from 0.5 wt% to 2.0 wt% were prepared by ball milling technique at a rotation rate of 300 r/min for 24 h under an argon atmosphere. Ball to powder mass ratio of 10:1 was considered as milling condition. Fig.1c and Fig.1d present SEM images of Ag-0.5wt% graphene composite powders fabricated by the ball milling process. As seen in Fig.1c and Fig.1d, the composite pow-

ders were flattened and welded together to form thin flakes by the repeated compressive impact forces between balls and composite powders. The graphene was embedded in the flake Ag powders. Fig.1e shows the XRD pattern of the Ag-0.5wt% graphene powders. We could obviously see the diffraction peak at  $26.5^\circ$ , which is due to the (002) plane of graphene, and the other four diffraction peaks of silver. No other diffraction peak was detected. This confirmed that no phase transition occurs between silver and graphene during the preparation and the raw materials are not oxidized or contaminated.

The milled composite powders were consolidated using double action compaction die with the low compaction pressures of 50, 100, 150 and 200 MPa at room temperature. The green compacts of the composites were sintered for 2 h at the temperature of 700, 750, 800 and 850  $^\circ\text{C}$  in a tubular furnace with a heating rate of 10  $^\circ\text{C}/\text{min}$  under a vacuum degree less than  $1 \times 10^{-3}$  Pa.

The apparent density of the Ag-graphene composite powders was measured by Scott volumeter method according to GB/T 1479.2-2011. The densities of the green and sintered composites were estimated by Archimedes principle and the results were averaged out over three independent measurements. The theoretical density of compacts was calculated from the simple rule of mixtures taking the fully dense values for silver ( $10.53 \text{ g}\cdot\text{cm}^{-3}$ ) and graphene ( $2.2 \text{ g}\cdot\text{cm}^{-3}$ ). Tensile tests were conducted on the AG-X100KN electronic universal testing machine with 0.5 mm/min loading speed at room temperature and three tensile samples were made for each composition.

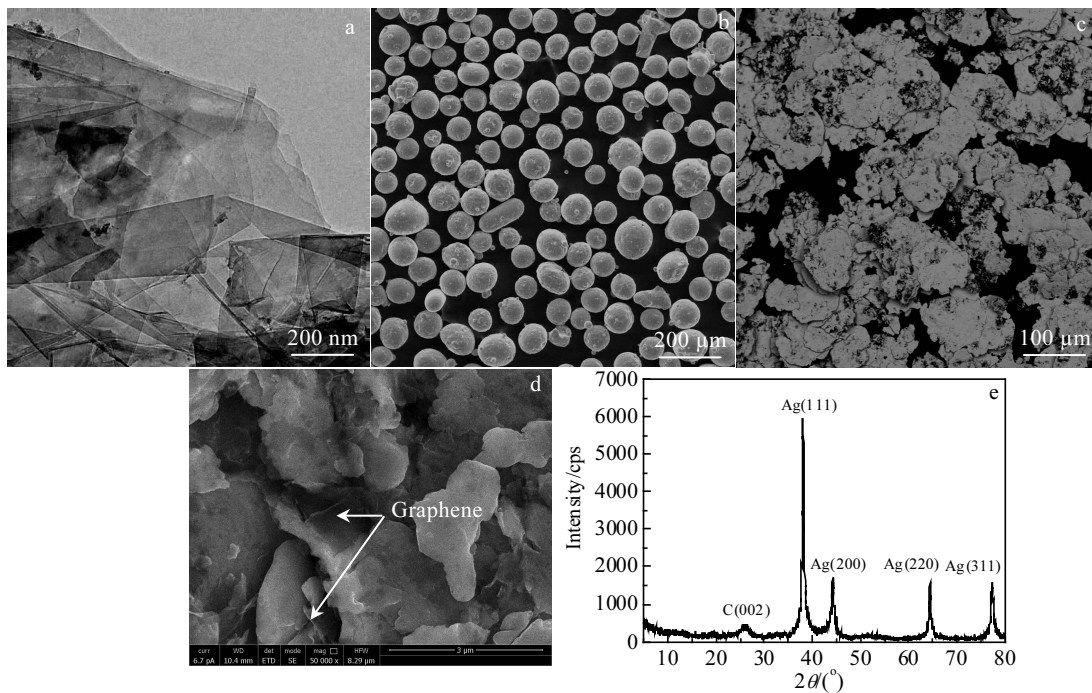


Fig.1 TEM image of graphene (a); SEM image of pure silver powders (b); SEM images of Ag-0.5wt% graphene powders after ball milling (c, d); XRD pattern of Ag-0.5wt% graphene powders (e)

## 2 Results and Discussion

### 2.1 Apparent density

The apparent density of the Ag-graphene composite powders is shown in Fig.2. The apparent density of the Ag-graphene composite powders increases with graphene content increasing up to 1.5 wt% and then decreases with graphene content increasing further. It is well known that plastic deformation is easy to occur in pure Ag powders. During ball milling, the shape of the Ag powder changes from spherical to flake and the graphene is embedded in the flake Ag powders (as shown in Fig.1c and Fig.1d).

The friction, which occurs during particles rearrangement, decreases due to the embedding of graphene, so the apparent density of Ag-graphene composite powders increases with graphene content up to 1.5 wt%. However, a sufficient surface area for the embedding process is not provided in the flake Ag matrix powders after graphene content up to 1.5 wt%, and particle rearrangement is denied by the graphene agglomeration, which cannot be embedded within the flake Ag powders. Moreover, the mixed composite powders including Ag and agglomerates of graphene shows high internal friction. Therefore, the apparent density of Ag-graphene composite powders decreases after graphene content up to 1.5 wt%. The content and agglomeration are the main problem for uniform distribution of graphene within the metal matrix<sup>[10]</sup>. In fact, graphene is highly prone to assemble owing to their nano-size effects and remarkable specific surface area, especially when a high amount of graphene are added, as shown in Fig.3.

### 2.2 Densification and compressibility

The relative density of the Ag-graphene composites compressed at varying compaction pressures is shown in Fig.4. The relative density of all Ag-graphene composites increases with the increase of compaction pressures, which is expected to occur due to particle rearrangement and the plastic deformation of Ag particles. The relative density of the composites is reduced with an increase in the graphene content from 0.5 wt% to 2.0 wt% under varying compaction pressures. The Ag-0.5wt% graphene composite exhibits excellent densification behavior for the same range of compaction pressures. It indicates that a greater amount of graphene addition is adverse to improving the compressibility of Ag-graphene composites.

The consolidation behavior of the Ag-graphene composite powders was evaluated by linear compaction equations proposed by Balshin which was suitable for low pressure (<300 MPa) and soft particles<sup>[16]</sup>. To analyze the compressibility behavior, the Balshin equation was used as follows.

$$\left(\frac{1}{D}\right) = k \ln P + B \quad (1)$$

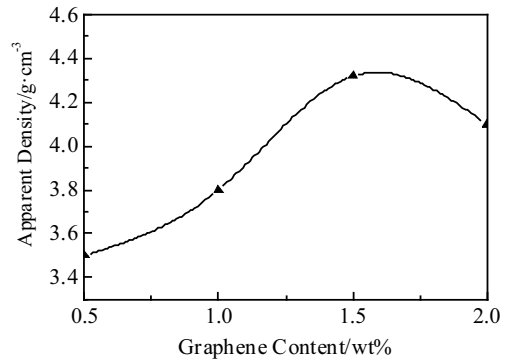


Fig.2 Apparent density of Ag-graphene composite powders with different graphene contents

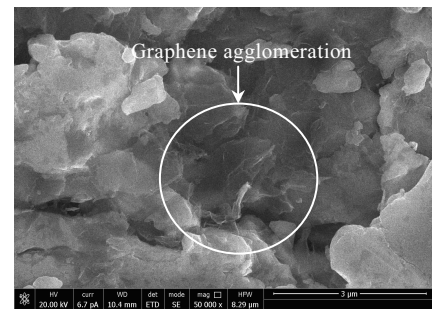


Fig.3 SEM image of graphene agglomeration in silver matrix of Ag-2.0wt% graphene composite powders

Where  $D$  is the relative density of compacted material and  $P$  is the applied pressure.  $k$  and  $B$  are fitting parameters. The parameter  $k$  is related to the plastic deformation capacity of the powder particles during compacting process. The parameter  $B$  represents the density without applied pressure, which is the apparent density. The Balshin equation gave the advantages of investigating the role of plastic deformation on the densification of the metal-based composites<sup>[17]</sup>. The compaction data of all Ag-graphene powders are fitted well to the Balshin equation, as shown in Fig.5. The densification parameter ( $K$ ) values increase with the increase of the graphene contents which indicate the increase of plastic deformation capacity and the decrease of the densification rate. The Ag-2.0wt% graphene composite powders have the highest  $K$  value, indicating its highest plastic deformation capacity and lowest densification rate.

### 2.3 Densification and sinterability

The densities of Ag-graphene composites with various contents of graphene sintered at varying sintering temperatures are listed in Table 1. The sinterability of the composites is enhanced with the increase of sintering tem-

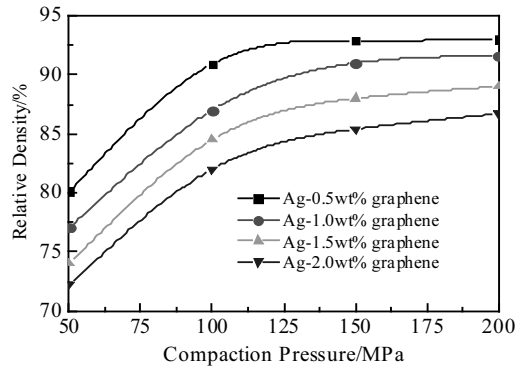


Fig.4 Compressibility curves of Ag-graphene composite powders after ball milling for 24 h

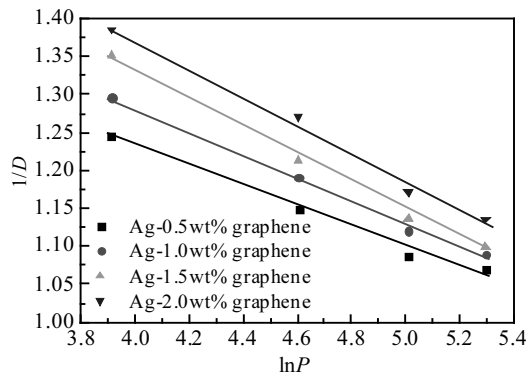


Fig.5 Balshin equation curves of Ag-graphene composites

peratures but decreases with the increase of graphene content. Sintered density mostly depends on the distance between powders in the particle reinforced composites<sup>[18]</sup>. When graphene B added to the Ag-graphene composites, the distance between Ag powders increases, and the sinterability is reduced. The agglomeration of the graphene reduces the sintered density of the Ag-graphene composites because the agglomeration regions act as a resistant barrier to Ag particle boundary diffusion during the sintering process, as illustrated in Fig.6.

It is observed that the highest relative density value is 97.94% for 850 °C sintered Ag-0.5wt% graphene composite, while the lowest value is 92.39% for Ag-2.0wt% graphene composite, as seen in Table 2. The relative density value of Ag-0.5wt% graphene and Ag-2.0wt% graphene is higher than and lower than that reported by Hao<sup>[19]</sup>, respectively. This indicates that excessive addition of graphene in present study significantly decreases the relative density of silver matrix composite.

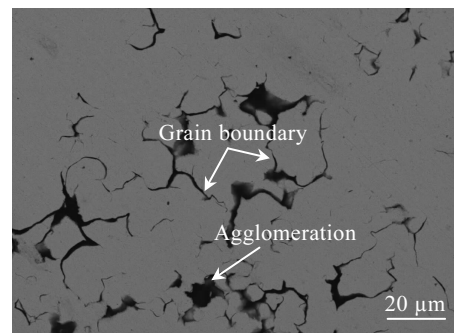


Fig.6 Microstructure of the sintered Ag-graphene composite

Table 1 Densities of Ag-graphene composites after sintering at different temperatures

Graphene content/wt%	Theoretical density/g·cm <sup>-3</sup>	Green density/g·cm <sup>-3</sup>	Density/g·cm <sup>-3</sup>			
			700 °C	750 °C	800 °C	850 °C
0.5	10.488	9.716	9.884	9.961	10.104	10.272
1.0	10.447	9.569	9.721	9.802	9.907	10.011
1.5	10.405	9.260	9.448	9.517	9.688	9.803
2.0	10.363	8.985	9.206	9.279	9.445	9.574

Table 2 Relative density of Ag-graphene composites

Graphene content/wt%	Relative density/%	Reference
0.5	97.94	-
0.5	94.87	[19]
1.0	95.83	-
1.5	94.21	-
1.5	94.80	[19]
2.0	92.39	-

The sinterability of the Ag-graphene composites could be evaluated by the following equation<sup>[20]</sup>.

$$\Phi = \frac{\rho_s - \rho_g}{\rho_{th} - \rho_g} \quad (2)$$

Where  $\rho_s$ ,  $\rho_g$  and  $\rho_{th}$  were the sintered, green and theoretical densities of the Ag-graphene composites, respectively. The sinterability of the Ag-graphene composites is shown in Fig.7. Sinterability of the Ag-graphene composites is reduced with the increase of the graphene content from 0.5 wt% to 2.0 wt% at varying sintering temperatures. From

Fig.7, it could be reaffirmed that the sinterability is positively correlated with the increase of the sintering temperature while negatively correlated with the increase of the graphene content. The Ag-0.5wt% graphene composite has the best sinterability, and its  $\Phi$  value at 850 °C is 0.72.

## 2.4 Mechanical properties

Fig.8 presents the stress-strain curves of pure Ag and Ag-graphene composites after sintering at 850 °C. In addition, the average values and errors of tensile strength and elongation of the three samples are listed in Table 3. At the initial stage of the curve, the tensile stress increases rapidly with the increase of strain and reaches its maximum value. Then, the curve experiences a platform area but drops at a certain strain (as shown in Fig.8). It could be seen that graphene shows excellent reinforced effect on mechanical strength of the Ag-graphene composite. Meanwhile, the addition of graphene decreases the ductility of the composites. With introducing 0.5 wt% and 1.5 wt% graphene, the tensile strength of Ag-graphene composites increases from 230 MPa to 244 MPa and 252 MPa, respectively. The Ag-0.5wt% graphene composite has a tensile strength of 230 MPa, ~67% higher than that of the Ag matrix, which indicates that graphene is a highly effective reinforcement in Ag matrix. However, the elongation of the composites decreases from 13.8% to 11.2% and 8.9%, respectively (as listed in Table 3). when only less than 1.5 wt% graphene is added into the Ag matrix, the enhancement ratio of mechanical strength produced by graphene significantly exceeds any other reinforcement, such as graphite, SnO<sub>2</sub> and Yb<sub>2</sub>O<sub>3</sub><sup>[21,22]</sup>. The result demonstrates that graphene has great potential as the most ideal reinforcement for silver matrix electrical contact materials.

Ag-graphene composites present unique and efficient enhancement, compared with conventional oxide particles and graphite enhanced silver-based composites. This may be resulted from dislocation pinning by the multiply wrinkled graphene and preventing crack propagation at interface junctions by good combination of graphene with the metal

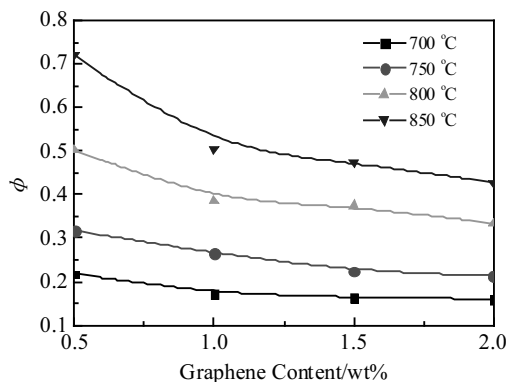


Fig.7 Curves of sinterability of Ag-graphene composites

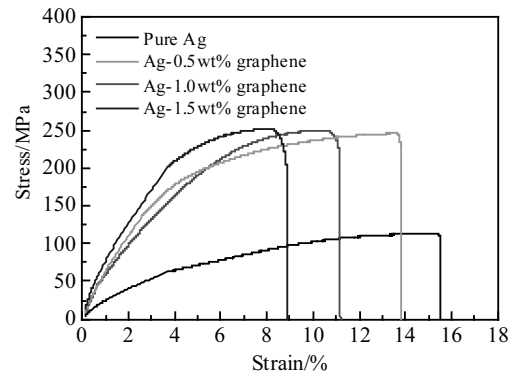


Fig.8 Stress-strain curves of Ag-graphene composites

Table 3 Tensile strength and elongation of the composites

Graphene content/wt%	Tensile strength/MPa	Elongation/%
0	108±3	15.6±0.2
0.5	230±3	13.8±0.2
1.5	244±3	11.2±0.2
2.0	252±3	8.9±0.2

matrix<sup>[23]</sup>. Although Rashad et al<sup>[24]</sup> and Chu et al<sup>[25]</sup> proposed some valuable and positive results in graphene reinforced metal-based composites, there still had a lot of unknown strengthening effect and influence factors which need to be explored. The strengthening mechanism of graphene reinforcement in silver-based composite will be comprehensively analyzed by the modified shear lag model and Hall-Petch relationship in our future research.

## 3 Conclusions

1) The apparent density of the Ag-graphene composites powders increases with graphene content increasing up to 1.5 wt% and then decreases with graphene content increasing further. When a high amount of graphene nanoplates are used in Ag matrix, graphene is highly prone to assemble owing to their remarkable specific surface area.

2) The compressibility of the composite powders decreases with the content of graphene up to 2.0 wt% under various compaction pressures from 50 MPa to 200 MPa. The compaction data are fitted well to the Balshin equation for studying the densification behavior. The addition of graphene decreases the densification rate of the composites.

3) The sinterability is positively correlated with the increasing sintering temperature while negatively correlated with the increasing graphene content. The Ag-0.5wt% graphene composite has the best sinterability, and its  $\Phi$  value at 850 °C is 0.72.

4) With introducing 0.5 wt% and 1.5 wt% graphene, the tensile strength of Ag-graphene composites increases from 230 MPa to 244 MPa and 252 MPa, respectively. The result

demonstrates that graphene has great potential as the most ideal reinforcement for silver matrix composites.

## References

- 1 Chu K, Wang X H, Li Y B et al. *Materials & Design*[J], 2018, 140: 85
- 2 Su Y, Zuo Q, Yang G et al. *Rare Metal Materials and Engineering*[J], 2017, 46(12): 3882 (in Chinese)
- 3 Murray J W, Rance G A, Xu F et al. *Journal of the European Ceramic Society*[J], 2018, 38(4): 1819
- 4 Li J H, Zhang X Z, Geng L. *Materials & Design*[J], 2018, 144: 159
- 5 Mohan V B, Lau K T, Hui D et al. *Composites Part B: Engineering*[J], 2018, 142: 200
- 6 Hwang J, Yoon T, Jin S H et al. *Advanced Materials*[J], 2013, 25: 6724
- 7 Yang W, Zhao Q, Xin L et al. *Journal of Alloys and Compounds*[J], 2018, 732: 748
- 8 Feng Y, Zhang M, Xu Y. *Carbon*[J], 2005, 43(13): 2685
- 9 Yin S, Zhang Z, Ekoi E J et al. *Materials Letters*[J], 2017, 196: 172
- 10 Varol T, Canakci A. *Metals and Materials International*[J], 2015, 21(4): 704
- 11 Sharma A, Sagar S, Mahto R P et al. *Surface and Coatings Technology*[J], 2018, 337: 12
- 12 Gao X, Yue H Y, Guo E et al. *Powder Technology*[J], 2016, 301: 601
- 13 Wang S, Wang S B, Xie M et al. *Precious Metals*[J], 2016, 37(2): 51 (in Chinese)
- 14 Yue H Y, Yao L H, Gao X et al. *Journal of Alloys and Compounds*[J], 2017, 691: 755
- 15 Ponraj N V, Azhagurajan A, Vettivel S C et al. *Surfaces and Interfaces*[J], 2017, 6: 190
- 16 Panelli R, Filho F A. *Powder Technology*[J], 2001, 114: 255
- 17 Jeyasimman D, Sivaprasad K, Sivasankaran S et al. *Powder Technology*[J], 2014, 258: 189
- 18 Jeyasimman D, Narayanasamy R, Ponalagusamy R. *Advanced Powder Technology*[J], 2015, 26: 1171
- 19 Hao X, Wang X, Zhou S et al. *Materials Chemistry and Physics*[J], 2018, 215: 327
- 20 Sivasankaran S, Sivaprasad K, Narayanasamy R et al. *Powder Technology*[J], 2010, 201: 70
- 21 Chen X H, Jia C C, Liu X B. *Rare Metals*[J], 2010, 29(4): 366
- 22 Zhang Z H, Jiang Y B, Chen Y T. *Journal of Alloys and Compounds*[J], 2017, 728: 719
- 23 Yan S J, Dai S L, Zhang X Y et al. *Materials Science and Engineering A*[J], 2014, 612: 440
- 24 Rashad M, Pan F, Yu Z et al. *Progress in Natural Science: Materials International*[J], 2015, 25(5): 460
- 25 Chu K, Jia C. *Physica Status Solidi A*[J], 2014, 211(1): 184

## 低压压制和真空烧结制备银-石墨烯复合材料的致密化行为

王 松, 郑婷婷, 谢 明, 李爱坤, 侯 攀

(昆明贵金属研究所 稀贵金属综合利用新技术国家重点实验室, 云南 昆明 650106)

**摘 要:** 为阐明低压压制成形和真空烧结制备的银-石墨烯复合材料的致密化行为, 通过 24 h 机械球磨制得石墨烯质量分数 0.5% 至 2.0% 的银-石墨烯复合粉末, 随后进行低压双向压制和真空烧结。通过测量复合材料压制后和烧结后的密度, 研究了不同成形压力和不同烧结温度工艺条件下复合材料的成形能力和烧结能力。结果表明: 银-石墨烯粉末的压制数据符合川北公夫方程。致密化系数( $K$ )值随石墨烯含量的增加而增大, 表明复合粉末抗塑性变形能力增大。银-0.5% 石墨烯复合材料具有最佳的烧结性能。石墨烯含量 1.5% 的复合材料具有较好增强效果的力学性能, 其抗拉强度达到 252 MPa。

**关键词:** 复合材料; 银-石墨烯; 致密化行为; 烧结性能; 低压压制

作者简介: 王 松, 男, 1986 年生, 硕士, 昆明贵金属研究所稀贵金属材料综合利用新技术国家重点实验室, 云南 昆明 650106, 电话: 0871-68328842, E-mail: songwipm@163.com